[12] Park, S. O., Lee, C. H., and Kang, K. M., "Naiver–Stokes Analysis of a Supersonic Flow over Moving Compression Ramp," AIAA Paper 2001-0568, 2001.

S. K. Aggarwal
Associate Editor

Modification of a Circular Cylinder Near Wake by a Rectangular Jet

D. M. Rooney* and M. S. Gaspin†
Hofstra University, Hempstead, New York 11549

Introduction

THE dynamics of a jet issuing into the wake behind various geometries in the presence of an upstream flow have been examined experimentally for a number of practical cases since Naudascher[1] first called attention to the phenomena occurring in the wakes of self-propelled bodies. Bradbury[2] contemporaneously measured the characteristics of turbulent plane jets exiting a thin slot at the trailing edge of an airfoil section, in the presence of an upstream flow of lower velocity than the jet. More recently, Serviente and Patel[3] have measured mean and turbulent velocity profiles behind an axisymmetric self-propelled body at various locations downstream of the jet nozzle. Several investigators have utilized less streamlined shapes as sources for the rear jet. Koutmos et al.[4] placed a square cylinder with a rear slot across a wind tunnel to determine the effect of injection ratio (jet to upstream velocity) on vortex shedding and recirculation patterns behind the square. Wood[5] employed an airfoil leading edge with an abrupt trailing edge and noted the effect of a jet on vortex formation and entrainment length of the shear layers. Zhdanov[6] followed by varying the width of the jet slot for a similar geometry.

Although wake phenomena behind circular cylinders in crossflow have been examined thoroughly, there has been little effort to examine the effect of a rear jet on that well-known wake structure. Duke et al.[7] executed a water channel flow visualization study with a high-speed jet exiting a spanwise slot in a circular cylinder, but made no detailed measurements within the wake. Although experiments with axisymmetric jets behind models approximating to submarines, or with slotted jets behind airfoils that shed light on jet flap performance have more direct utility, nevertheless examination of the circular cylinder with rear-exiting jet can draw attention to similarities as well as differences in the response of bluff body wakes vis-à-vis streamlined body wakes in the presence of a jet. It is the purpose of the present Note to draw attention to the salient features of this particular jet–wake interaction.

Experimental Apparatus

Experiments were undertaken in a Hofstra University subsonic wind tunnel facility with a circular test section of 30.48-cm diam. Test cylinders with endplates spanned the tunnel width and featured a spanwise slot at midheight measuring $H = 25.4$ mm in length by $h = 0.635$ mm in width. A jet was produced by compressed air at 414 kPa (60 psi), and the jet flow was controlled by a regulator that produced volumetric flow rates ranging from 0 to 2400 l/h. The limited spanwise length of the slot necessarily produced a three-dimensional jet, the properties of which were measured along the major and minor axes at several locations downstream of the exit plane. Attention was primarily focused on data taken at the middle of the major axis of the slot because the mass flow rate of the jet was greatest around that height, thereby permitting the best comparison of the effect of a rear jet on a circular cylinder wake.

Two cylinders, one of $D = 6.35$ mm diameter and one of $D = 12.7$ mm diameter, were used during the test program. A minimum of nine test cases were run for each cylinder at two locations: three diameters and five diameters behind the central longitudinal axis of each of the cylinders. First the wake characteristics for an upstream velocity impinging on the cylinder with no rear jet were measured, then the wake produced by the jet alone at each of at least four jet flow rates employed, and then the wake produced by the jet in conjunction with the upstream flow at each of those jet flow rates. The upstream velocity was kept constant throughout the test program at $U_0 = 10.0$ m/s so that the Reynolds number based on cylinder diameter was either 4×10^3 or 8×10^3, for the smaller and larger cylinder, respectively. A nominal jet velocity V_j was obtained by dividing the volumetric flow rate as indicated on an Omega FL-210 flow meter by the cross-sectional area of the slot. Because of unsought differences in the machining of the slots, the jet profiles for the two cylinders differed. The smaller diameter cylinder produced a jet that was more concentrated at midheight, with little mass flow exiting at the upper and lower edges of the slot. Vertical scanning also showed some evidence of the saddlebacked velocity profiles that Quinn et al.[8] have documented to exist along the major axis of rectangular slots from which jets issue. For a representative flow rate, the velocity decreased along the major axis of the smaller cylinder to 50% of its maximum value over a 5-mm span and to 20% of its maximum value over an 8-mm span, when measured five diameters downstream of the cylinder axis. For the larger cylinder, the decrease to 50% of the maximum velocity occurred over a 14-mm span and to 20% of the maximum over a 22-mm span at five diameters downstream. At a comparable absolute distance downstream (three diameters for the larger cylinder being 31.7 mm from the slot, and five diameters downstream of the smaller cylinder measured 28.6 mm from the slot) the large cylinder velocity decreased to 50% over a 16-mm span and to 20% over a 22-mm span. Clearly the smaller cylinder jet was narrower vertically, but it expanded horizontally more rapidly at midheight. Despite these differences, it was decided to examine both cylinders because distinct jet structures would interact with a given cylinder wake, and any resulting dissimilarities in the combined flow wake could be analyzed in light of the given jet profile.

Both mean local velocity and turbulence intensity were measured at 1-mm intervals over a 40 mm length, 20 mm on either side of the cylinder center, using a hot-wire probe attached to a TSI Model 1054B constant temperature linearized anemometer. The temperature of the air jet and the wind-tunnel flow were measured by to be within 0.3°C of each other, so that no thermal biasing to the hot-wire readings occurred. Data passed through a filter to an rms voltmeter, which registered the rms fluctuations on the mean probe signal, and to an oscilloscope, where a visual signal was observed. A data acquisition system averaged and recorded readings for rms and mean velocity, and a Bruel–Kjaer spectrum analyzer monitored vortex shedding frequencies. Figure 1 shows the experimental setup.

Results and Discussion

The results are presented in dimensionless format with the relative magnitude of the jet characterized by a bleed coefficient $C_q = hV_j/DU_0$, the ratio of the jet flow rate to the rate of freestream flow through the same span H occupied by the slot, for a given diameter D. Distances behind and across the wake of the cylinder are nondimensionalized by the diameter. Hence, mean velocity and turbulence intensity profiles were constructed as a function of relative distance (z/D) across the cylinder wake at streamwise distances $x/D = 3$ and 5. The 95% confidence interval in mean freestream

Received 24 July 2002; revision received 16 September 2002; accepted for publication 16 September 2002.

*Associate Professor, Department of Engineering. Member AIAA.

†Undergraduate Research Assistant, Department of Engineering; currently Undergraduate Student, Department of Mechanical and Aerospace Engineering, Cornell University, Ithaca, NY 14853.

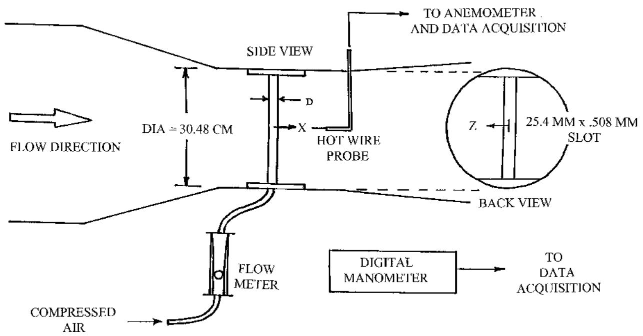

Fig. 1 Experimental setup.

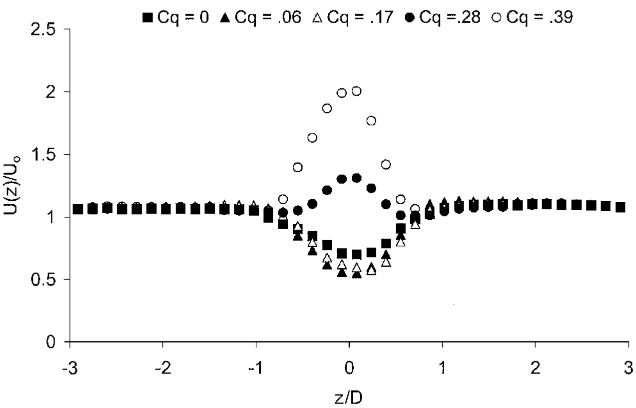

Fig. 2 Mean velocity profiles at midheight of slot (combined flow) at *x/D* = 3 and *h/D* = 0.08.

velocity readings was ±0.3 m/s. In the flowmeter readings were ±6% at the lower flow rates tested and diminished with increasing flow rate. Consequently, the maximum uncertainty in the bleed flow coefficient C_q was 6.7%.

Figure 2 shows representative results obtained with the 6.35-mm-diam cylinder ($h/D = 0.08$) at a distance $x/D = 3$ behind the cylinder axis. It is apparent that, for a bleed coefficient above some threshold value, the combined mean flow represents a near combination of a core jet flow (with slightly reduced maximum velocity) in the range $-1 < z/D < +1$, with the upstream velocity operative in the outer region. This result was noted by Serviente and Patel[3] for an axisymmetric jet emanating from a streamlined body when $V_j/U_0 = 1.35$, but only at fractions of a nozzle distance downstream of the jet exit plane. Of more interest in the present results is that, for low bleed coefficients, the velocity defect in the wake was actually greater than when no jet was present. The centerline velocity in the wake was $0.70U_0$ with no jet but decreased to $0.55U_0$ in the presence of a jet, which by itself had generated a velocity of magnitude $0.40U_0$. The addition of a jet also diminished the magnitude and the width of axial turbulence from the maximum values occurring when no jet was present, producing the most quiescent wake at bleed coefficients in the range of $C_q = 0.17$–0.28, before increasing again at a higher tested bleed coefficient. The jet alone exhibited progressively higher turbulence levels over a wider wake with increasing bleed coefficient, and so the combined flow displayed a highly nonlinear response to the addition of a jet.

For the larger cylinder, the maximum bleed coefficient examined was $C_q = 0.19$; thus, not surprisingly the velocity defect in the wake was never offset by the momentum supplied by the jet. In fact, the results showed that whereas the upstream flow alone again registered a centerline velocity of $0.70U_0$, application of a jet corresponding to $C_q = 0.08$ decreased the centerline velocity to $0.3U_0$, and by itself that jet flow rate produced a centerline velocity of $0.55U_0$.

The situation slightly farther downstream at $x/D = 5$ was less dramatic as the jet widened, and its maximum centerline velocities diminished. The jet-only maximum velocities were $1.90U_0$ for the small and $1.05U_0$ for the large cylinder. The negative effects of introducing a low jet flow rate into the wake could still be seen, particularly behind the smaller cylinder, where the combined centerline velocity, which was measured to be $0.88U_0$ for no jet, fell to $0.60U_0$ for a bleed coefficient $C_q = 0.17$.

Koutmos et al.[4] found that, for the wake behind a square with central injection, the primary air stagnation point (behind the recirculation region) moved downstream with increasing low jet velocities and then reversed direction above a critical ratio because of a reduction of entrainment of wake fluid. Their experiments further showed that the stagnation point always occurred before $x/D = 3$. For a circular cylinder wake, one would expect the stagnation point to occur nearer the cylinder. Figure 3 shows the variation of the mean centerline velocity with increasing bleed coefficient for the larger cylinder at the two x/D locations. The measured decrease followed by an increase in centerline velocities for increasing bleed coefficient is explicable by the phenomenon of an expanding and then contracting recirculating region directly behind the cylinder.

Relative wake widths W/D (or actual wake width divided by cylinder diameter, henceforth referred to simply as wake width) were determined by measuring the distance across the wake between points where turbulence intensity is one-half its maximum value (the $r_{1/2}$ method). Repeated measurements yielded results consistent within ±1.5 mm in wake widths, for a 95% confidence interval in W/D of ±0.23 for the smaller cylinder and ±0.12 for the larger cylinder. The wake width at a given x/D location should, of course, be independent of cylinder diameter for the upstream flow acting

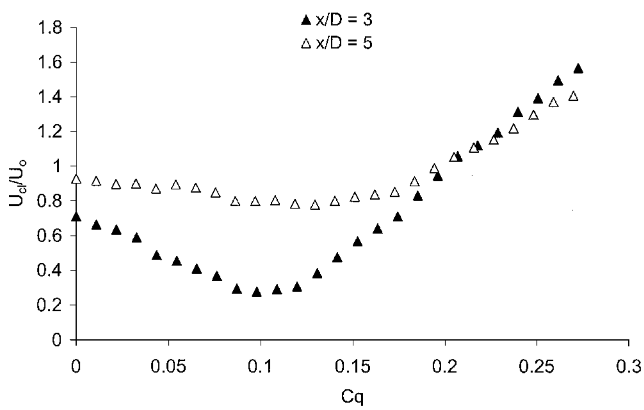

Fig. 3 Centerline mean velocity variation for *h/D* = 0.04 as a function of bleed coefficient.

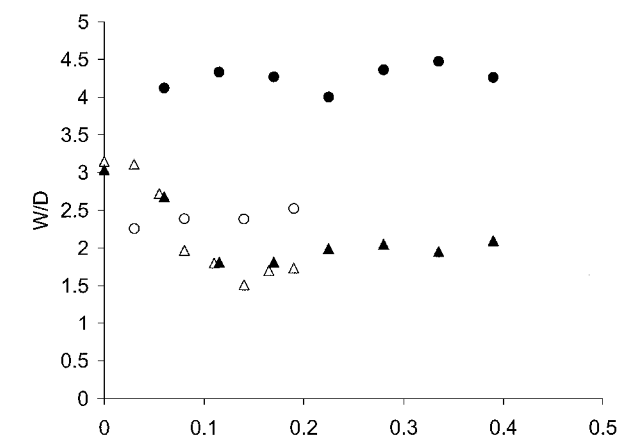

Fig. 4 Relative wake width at midheight of slot at *x/D* = 5: ●, jet flow, *h/D* = 0.08; ▲, combined flow, *h/D* = 0.08; ○, jet flow, *h/D* = 0.04; and △, combined flow, *h/D* = 0.04.

alone. However, for the jet acting alone, the slot geometry governs the growth of the wake. Given the aforementioned difference noted in the jets issuing from the two ostensibly similar slots, one would expect a complex relation between wake width and bleed coefficient for the cylinders examined. Reference to Fig. 4 in fact shows that for the smaller ($h/D = 0.08$) cylinder, the jet-only wake exceeded the upstream-only wake at $x/D = 5$, whereas for the larger cylinder the upstream-only wake was greater than the jet-only wake. A jet wake of 4.2 behind the smaller cylinder contracted to half that magnitude in a combined flow, whereas the upstream-alone case generated a wake width of 3.1. The contracting effect at higher bleed coefficients was less pronounced for the larger cylinder diameter, but still significant: For $C_q = 0.14$, values dropped from 2.3 for the jet alone to 1.5 for the combined flow. However, most interesting, the results for both cylinders superposed on one another, suggesting that in spite of differences in jet profiles, the bleed coefficient alone is a good predictor of wake width downstream of the jet exit.

Finally vortex shedding activity was observed at a station 10 diameters downstream and 1–2 diameters off the streamwise centerline of each cylinder. The differences in jet geometry had no effect on the persistence of organized shedding, which remained the same as for the upstream-only flow up to $C_q = 0.06$ and then split into a broader range with two identifiable dominant frequencies up to $C_q = 0.11$ before disappearing for higher bleed coefficients. The jet flow had become strong enough to prevent flow from being swept across the wake central axis, as occurs in a vortex formation region. Without that mixing, alternate shedding ceased to exist.

Conclusions

Injection of a jet into the wake produced by an upstream flow around a circular cylinder alters its well-understood dynamics, which now become a function of the geometry of the jet as well as its relative magnitude. Whereas previous investigators who focused solely on the momentumless wake behind a streamlined body found augmentation of the near wake by axisymmetric jet injection, the present paper notes a greater velocity defect in the near wake of a bluff body in the presence of a relatively low jet flow rate. The presence of a jet also decreases the wake width, which depends more on the magnitude of the bleed coefficient than the configuration of the jet. Vortex shedding activity is likewise more a function of bleed coefficient than of jet geometry.

References

[1]Naudascher, E., "Flow in the Wake of Self-Propelled Bodies and Related Sources of Turbulence," *Journal of Fluid Mechanics*, Vol. 22, Pt. 4, 1965, pp. 625–656.

[2]Bradbury, L. J. S., "The Structure of a Self-Preserving Turbulent Plane Jet," *Journal of Fluid Mechanics*, Vol. 23, Pt. 1, 1965, pp. 31–64.

[3]Serviente, A. I., and Patel, V. C., "Wake of a Self-Propelled Body, Part 1: Momentumless Wake," *AIAA Journal*, Vol. 38, No. 4, 2000, pp. 613–619.

[4]Koutmos, P., Mavridis, C., and Papiliou, D., "A Study of Unsteady Wake Flows Past a Two Dimensional Square Cylinder with and Without Planar Jet Injection into the Vortex Formation Region," *Applied Scientific Research*, Vol. 55, No. 3, 1996, pp. 187–210.

[5]Wood, C. J., "Visualization of an Incompressible Wake with Base Bleed," *Journal of Fluid Mechanics*, Vol. 29, Pt. 2, 1967, pp. 259–272.

[6]Zhdanov, V. L., "Effect of Jet Bleed Out of the Base of a Model on the Base Pressure and Frequency Characteristics of Wake Flow," *Journal of Engineering Physics and Thermophysics*, Vol. 71, No. 4, 1998, pp. 627–632.

[7]Duke, R., Shrader, B., and Mo, J., "Effects of a Rear Stagnation Jet on the Wake Behind a Cylinder," *AIAA Journal*, Vol. 31, No. 9, 1993, pp. 1727–1729.

[8]Quinn, W. R., Pollard, A., and Masters, G. F., "Mean Velocity and Static Pressure Distribution in a Three-Dimensional Turbulent Freejet," *AIAA Journal*, Vol. 23, No. 6, 1985, pp. 971–973.

W. J. Devenport
Associate Editor

Rotating Multilayered Cylindrical Shells to Impact Loading

S. W. Gong* and K. Y. Lam†
Institute of High Performance Computing, Singapore 117528, Republic of Singapore

Introduction

IMPACT on multilayered shell structures has been a subject of considerable interest and concern in recent years. Christoforou and Swanson[1] formulated an analytic solution to the problem of simply supported, orthotropic cylindrical shells subjected to impact loading. In their analysis, the deceleration of the impacting mass was used to estimate the impact force. Gong et al.[2] adopted Christoforou and Swanson's approach and undertook analyses of laminated cylindrical shells subjected to impact. In their work, contact deformation was considered, and an analytic function describing it was proposed and incorporated into the analysis. Recently, Gong et al.[3] presented solutions for the problems of functionally graded material (FGM) cylindrical shells subjected to low-velocity impact, and Gong and Lam[4] examined the effects of structural damping on impact response.

None of the preceding studies, however, have dealt with rotating multilayered shells subjected to impact loading. Rotating shells have a wide range of engineering applications, such as in the high-speed centrifugal separator, high-power aircraft jet engine, and the drive shaft of gas turbine, motor, rotor system. With the use of composite material in rotating shell structures, their engineering applications have been extended and improved further.[5] Therefore, a comprehensive study and understanding of transient response of a rotating multilayered shell to impact is essential. The present work addresses this and presents an analytic solution to the problem of a rotating composite shell to impact loading.

Governing Equations

Consider a multilayered cylindrical shell rotating about its symmetrical and horizontal axis at a constant angular speed Ω, as shown in Fig. 1. The shell has a mean radius of R, length of L, and thickness of h. The reference surface of the shell is taken to be at its middle surface, where an orthogonal coordinate system (x, θ, z) is fixed. The displacements of the cylinder in the x, θ, and z directions are defined by u, v, and w, respectively. For the rotating cylindrical shell subjected to a distributed load q_n that is normal to the reference surface, the governing equations of motion for the rotating cylindrical shell can be expressed as

$$\frac{\partial \boldsymbol{N}_x}{\partial x} + \frac{\partial \boldsymbol{N}_{x\theta}}{R\partial \theta} + \tilde{N}_\theta\left(\frac{1}{R^2}\frac{\partial^2 u}{\partial \theta^2} - \frac{1}{R}\frac{\partial w}{\partial x}\right) = \rho h \frac{\partial^2 u}{\partial^2 t} \tag{1}$$

$$\frac{\partial \boldsymbol{N}_{x\theta}}{\partial x} + \frac{\partial \boldsymbol{N}_\theta}{R\partial \theta} + \frac{\partial \boldsymbol{M}_{x\theta}}{R\partial x} + \frac{\partial \boldsymbol{M}_\theta}{R^2\partial \theta} + \frac{\tilde{N}_\theta}{R}\frac{\partial^2 u}{\partial x \partial \theta} = \rho h\left(\frac{\partial^2 v}{\partial^2 t} + 2\Omega\frac{\partial w}{\partial t} - \Omega^2 v\right) \tag{2}$$

Received 23 August 2001; revision received 10 July 2002; accepted for publication 3 September 2002.

*Principal Research Engineer, 1 Science Park Road, Number 01-01 The Capricorn, Singapore Science Park II. Member AIAA.

†Director, 1 Science Park Road, Number 01-01 The Capricorn, Singapore Science Park II.